VALIDATION OF NUMERICAL APPROACHES FOR ELECTROMAGNETIC CHARACTERIZATION OF MAGNETIC RESONANCE RADIOFREQUENCY COILS

**Riccardo Stara[1, 2, *], Nunzia Fontana[2, 3],
Gianluigi Tiberi[3, 4], Agostino Monorchio[2, 3],
Giuliano Manara[2, 3], Maria Alfonsetti[5, 6],
Angelo Galante[5, 6], Assunta Vitacolonna[5, 6],
Marcello Alecci[5, 6], Alessandra Retico[2],
and Michela Tosetti[7]**

[1]Dipartimento di Fisica, Università di Pisa, Largo B. Pontecorvo 3, Pisa 56127, Italy

[2]Istituto Nazionale di Fisica Nucleare, Sezione di Pisa, Largo B. Pontecorvo 3, Pisa 56127, Italy

[3]Dipartimento di Ingegneria dell'Informazione, Università di Pisa, Via G. Caruso 16, Pisa 56122, Italy

[4]Fondazione IMAGO7, Viale del Tirreno 341, Calambrone, Pisa 56128, Italy

[5]Dipartimento Medicina Clinica, Sanità Pubblica, Scienze della Vita e dell'Ambiente, Università degli Studi dell'Aquila, Via Vetoio 10, Coppito, L'Aquila 67100, Italy

[6]Istituto Nazionale di Fisica Nucleare, Laboratori Nazionali del Gran Sasso, S.S. 17 bis km 18910, Assergi, L'Aquila 67010, Italy

[7]IRCSS Fondazione Stella Maris, Viale del Tirreno 341, Calambrone, Pisa 56128, Italy

Abstract—Numerical methods based on solutions of Maxwell's equations are usually adopted for the electromagnetic characterization of Magnetic Resonance (MR) Radiofrequency (RF) coils. In this context, many different numerical methods can be employed, including time domain methods, e.g., the Finite-Difference Time-Domain (FDTD), and frequency domain methods, e.g., the Finite Element Methods (FEM) and the Method of Moments (MoM). We provide

a quantitative comparison of performances and a detailed evaluation of advantages and limitations of the aforementioned methods in the context of RF coil design for MR applications. Specifically, we analyzed three RF coils which are representative of current geometries for clinical applications: a 1.5 T proton surface coil; a 7 T dual tuned surface coil; a 7 T proton volume coil. The numerical simulation results have been compared with measurements, with excellent agreement in almost every case. However, the three methods differ in terms of required computing resources (memory and simulation time) as well as their ability to handle a realistic phantom model. For this reason, this work could provide "a guide to select the most suitable method for each specific research and clinical applications at low and high field".

1. INTRODUCTION

Since the emergence of *in-vivo* Magnetic Resonance Imaging (MRI) and Spectroscopy (MRS) there has been a great interest in predicting and characterizing the electromagnetic behavior of RF coils and their interaction with the sample under investigation.

Several clinical MRI/MRS applications require a careful selection and design of the RF coil, to optimize the RF spatial distribution and sensitivity.

For one or two channel systems the most common solutions are: i) the birdcage coil [1, 2] and the TEM resonator [3], which have become the standard for volume RF coils; ii) optimized surface RF coils capable of improved performance in reduced field of view [4–6].

As frequency increases, RF fields strongly interact with the sample [7, 8], i.e., the human tissues, making quasi-static approaches no more reliable for electromagnetic characterization. Moreover, the complex interactions between coils and biological sample cannot be solved by using analytical methods: numerical methods based on solutions of Maxwell's equations are mandatory [9]. In this context, many different numerical methods can be employed, including the Finite-Difference Time-Domain (FDTD) [10–13], the Finite Element Methods (FEM) [14–16] and the Method of Moments (MoM) [17–20].

FDTD, or its version involving the integral form of Maxwell's equations in time domain, i.e., the Finite Integration Technique (FIT), has been widely used for electromagnetic characterization of low and high field MR RF coils loaded with human-like phantoms. However, when applied to volume coils having multi-mode resonances, it suffers convergence problems. To overcome this difficulty many authors adopted a simplified geometry (without capacitors) driven at the desired RF frequency, according to the appropriate phase and

amplitude distribution of line currents [21, 22]. However, this approach cannot take into account the effects of high-order modes, leading to an under-estimation of the Specific Absorption Rate (SAR) [23]. FDTD has also some problems when dealing with structures having small radius of curvature, i.e., the rods or tube legs of volume TEM resonators or birdcage coils.

Conversely, FEM and MoM can mesh accurately the latter structures, but suffer in treating human-like models with high degree of inhomogeneity in terms of dielectric parameters and conductivity.

Concerning memory requirement, FEM methods requires a capacity that scales proportional to the complexity of the geometry, the frequency and the size of the surrounding space (i.e., for electrically small objects the surrounding space has to be very large). On the other hand, in MoM the memory requirement scales proportional to the geometry and the frequency, being the induced currents the unknowns of the problem (source method).

From this brief and preliminary overview, it is possible to point out that each one of the above mentioned numerical techniques permits the electromagnetic characterization of low and high field MR coil, each one having its own advantages and limitations. However, to the best of our knowledge, a quantitative comparison of RF coil simulation performances and a detailed evaluation of advantages and drawbacks is not available, rendering the choice of the simulation method often difficult and, eventually, not optimal.

The present work aims to providing some practical guidelines for choosing the best simulation algorithm depending on the specific problem.

2. METHODS AND MATERIALS

2.1. Numerical Methods: Theory

For time domain numerical simulation we used the FIT [24], which is implemented in CST (Computer Simulation Technology AG, Germany) MW Studio. The methodology of FIT is similar to the traditional Finite Differential Time Domain (FDTD) [25, 26]. While in FDTD the differential form of Maxwell equations is solved, in FIT the integral form of Maxwell's equations is solved. As in the traditional FDTD, a spatial and a time discretization of the Maxwell's equations are performed.

The FIT allows the simulation of a structure behavior in a wide frequency range in a single run. It allows the simulation of devices with open boundaries or large dimensions. Problems with complex and inhomogeneous structures can be numerically analyzed.

However, memory requirement scales proportional to the geometry, the frequency and the size of the surrounding space used as boundaries for terminating the domain and for simulating the free-space. By using the Perfect Matched Layer (PML) absorbing boundaries [26, 27], an automatic minimum distance from the structure (which is a fraction of the wavelength) is added. The latter distance used by the CST MW solver is approximately equal to $\lambda/8$, where λ is the wavelength at the central frequency of the frequency range chosen for the simulation. For electrically small objects, as most of the RF coils at high field are, the minimum distance is large compared to the size of the RF coil and, as consequence, the computational domain is large.

For frequency domain numerical simulation we used a Method of Moment [26], implemented in FEKO environment (EM Software & Systems, South Africa) and a Finite Element Method developed in the frequency domain of CST MW Studio. The main numerical effort in MoM analysis is the inversion of a dense matrix. While MoM is indicated for simple and homogeneous loads, e.g., cylinders and spheres, it is not appropriated for stratified or heterogeneous samples. Because the MoM is a source method (i.e., only the structure under test is discretized and no computational domain sampling is required) the computing time is shorter than for a FIT analysis.

In the FEM analysis Maxwell's equation are solved in the frequency domain. A spatial discretization of the computational domain is carried out by creating a tetrahedral grid, choosing the size of the mesh cell equal to $\lambda/10$ at least. The main onerous calculation for FEM analysis is the inversion of the matrix: however this matrix is sparse, so the inversion is easier if compared to a MoM analysis.

We thus conclude that FEM and MoM are both suited for the electromagnetic analysis of electrically small objects.

2.2. Geometrical Models of the MR Coils and Loads

Two RF surface coils and one volume RF coil have been constructed and analyzed. The first design is a Figure of Eight (Fo8) RF surface coil [5].

Figure 1(a) shows the Fo8 which has been constructed with copper strips of width 4 mm and thickness 100 μm. We modeled a circular Fo8 coil as reported in [5] having diameter of 10 cm and the gap between the two parallel linear currents elements of 1 cm. The geometry of the Fo8 RF coil is not fully planar: in order to avoid the short circuit between the two arms, a bridge has been built (as shown in the Figure 1(a) insert). The coil lies on a 1.6 mm thick FR4 substrate. In order to reach the tuning of the coil at 63.87 MHz one capacitor of 7.2 pF has been placed in parallel with the coil conductor path. A matching circuit
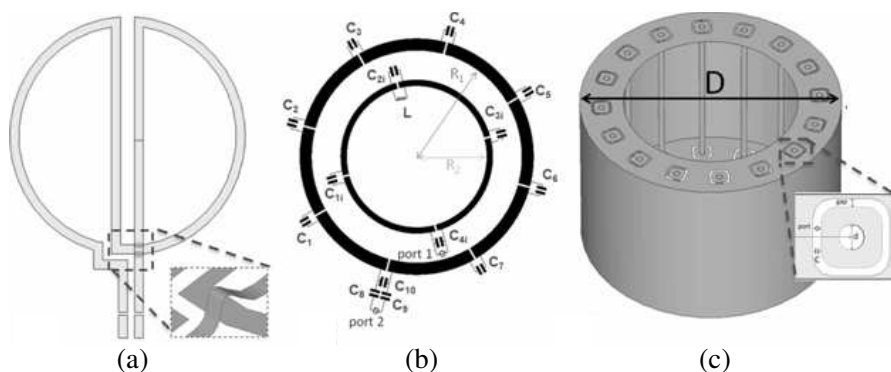
Figure 1. MRI RF coils simulated and experimentally tested: (a) Fo8; (b) dual-tuned ^{1}H/^{31}P surface coil; (c) TEM coil.

with one parallel capacitor of 120 pF and two series capacitors of 15 pF have been used.

Additionally, a dual tuned ^{1}H/^{31}P RF surface coil for MRI and MRS at 7 T has been developed and tested on the workbench. As shown in Figure 1(b), the design of the dual tuned RF coil consists of two concentric loops, with radius $R_1 = 4.5$ cm and $R_2 = 3$ cm for the outer and the inner loop, respectively. The external loop has been constructed with a copper strip of width 0.5 cm and the internal one with width of 0.25 cm. The strip thickness was equal to 35 µm in both cases. The loops lie on a Duroid substrate of thickness 1 mm. In order to tune the outer loop coil at 298 MHz (the proton resonance frequency at 7 T) and to reduce the intensity of the electric field within the sample, 7 capacitors have been placed in series with the outer loop ($C_{1-7} = 12$ pF and $C_{3-4} = 10$ pF) (see Figure 1(b)). The matching network for the outer loop comprised a parallel capacitor of $C_{10} = 0.5$ pF and two series capacitors of $C_{8-9} = 12$ pF [28].

The inner RF loop coil was tuned at 120.64 MHz (the phosphorus resonance frequency at 7 T) by using two capacitors ($C_{1i} = 18$ pF and $C_{3i} = 21.6$ pF) in series with the loop (Figure 1(b)). A parallel capacitor $C_{4i} = 120$ pF has been used for the matching. In order to decouple the two loops, a first order trap circuit, tuned at 298 MHz with $C_{2i} = 7.2$ pF and a $L = 39$ nH inductance has been placed in series with the inner loop [6]. The gap for the insertion of the capacitors has been chosen equal to 1 mm.

Finally, a TEM RF volume coil has been designed, built and tested for ^{1}H MRI/MRS at 7 T. The TEM RF coil consists (see Figure 1(c)) of 16 cylindrical copper legs (diameter of 6 mm; height of 15.8 cm)

surrounded by a cylindrical copper shield (diameter $D = 24$ cm; height of 15.8 cm). The distance between the shield and the center of the legs is 2 cm. In order to reach the resonance frequency of mode $M = 1$ of the TEM coil at approximately 298 MHz, a total of 32 capacitors $C = 2.1$ pF have been placed on the top and bottom end of the coil.

2.3. Numerical Models of MR Coils and Loads

We made a preliminary analysis of the coils with and without the presence of the dielectric substrates (FR4, Duroid, Plexiglass) into the geometry. We noticed that the results obtained in the two cases presented an excellent agreement. Thus, since the presence of the substrate produces a longer simulation time, its effect was neglected in all the subsequent numerical analyses.

The time domain analysis of the RF coils with and without the presence of the load has been performed by using FIT. In time domain, we first applied the automatic hexahedral mesh used by the solver which considers the maximum length of mesh cells equal to $\lambda_0/10$ in the free space and equal to $\lambda/10$ in the medium having a given permittivity (λ_0 is the wavelength at the central frequency of the frequency sweep used for the simulation).

Because the computational domain obtained for these structures is large, the automatic sampling made by the solver was not fine enough. For this reason, we refined the automatic hexahedral mesh in order to closely fit the geometry of the RF coils. The mesh refinement has been developed in order to fit the geometry of the RF coils in each direction (x, y, z) with three mesh cells at least: in the Fo8 RF coil case we refined the mesh on the rings, the arms and more closely on the profile of the bridge; in the dual-tuned RF coil case we refined the mesh on each loop. The complexity of the geometry made the mesh refinement for the TEM RF coil the most challenging. We performed the mesh in order to fit each leg of the coil and the shield with three mesh cells at least in each direction (x, y, z).

In the case of FEM analysis, first we choose a tetrahedral mesh in order to closely fit the geometry of the RF coils. Afterwards, an automatic adaptive tetrahedral mesh has been performed for each RF coil in order to increase the accuracy of the results.

In the case of MoM analysis the mesh is triangular with a density chosen to closely fit the geometry of the coils. An adaptive meshing has been used for the MoM analysis too, in order to increase the accuracy of the results.

The surface RF coils have been matched and tuned using a cylindrical phantom as load, with electric conductivity $\sigma = 0.686\,\Omega^{-1}\,\mathrm{m}^{-1}$ and relative permittivity $\epsilon_r = 79$ selected to simulate

the human muscle at 7 T [21]. The cylindrical phantom has a radius equal to 5.5 cm and height equal to 23 cm. This choice allows to directly compare the different simulation schemes, since MoM can hardly manage inhomogeneous loads. The same phantom has been used in all the experiments described here.

For RF coils the simulation must be able to provide the following information: the resonance frequency (i.e., the value of the tuning capacitors), the matching condition (i.e., the value of the capacitors in the matching network), and the distribution of the electric and magnetic fields. The S parameter simulation can be useful in the prototyping stage of the coils, whereas the electromagnetic field simulation is needed both before and after the realization of the coils, for example to evaluate the SAR and the magnetic field B_1 distribution.

Numerical simulations on the CST environment of the Fo8 and dual-tuned RF coils have been performed on an Intel i7 920 with 12 Gb of RAM memory, whereas the TEM RF coil simulation has been performed on an Intel i7 950 with 24 Gb of RAM memory. The MoM simulations of all RF coils have been performed on a Intel i7 980x with 12 Gb of RAM.

3. RESULTS AND DISCUSSION

3.1. Figure of Eight RF Coil

The first simulation refers to the loaded and unloaded Fo8 surface coil for MRI at 1.5 T. The load is displaced by 5 mm from the RF coil plane, as shown in Figure 2(a).

Regarding the evaluation of tuning and matching conditions, Table 1 shows the difference between the three simulation methods and the experimental results. Figure 2 shows a comparison between the maps of the magnetic and electric RF field obtained by the three simulation methods.

Table 1. Comparison between measurements and simulations for the Fo8 RF coil tuned at 64 MHz (1.5 T).

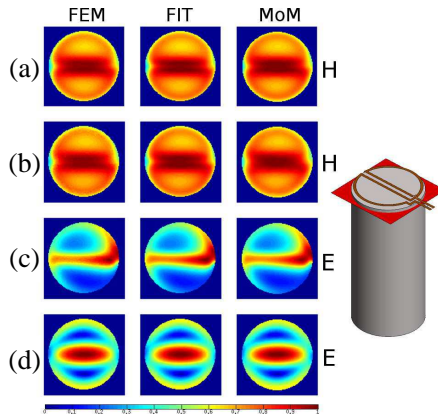| Quantity	Measure	MoM	FEM	FIT
Frequency	63.94 MHz	0.3%	2%	2%
Matching	−24 dB	0.2%	0.4%	0.4%
Simulation time	/	25 min	2 h 15 min	36 h 25 min
Peak RAM used	/	1.7 Gb	7.19 Gb	0.78 Gb
No. mesh cells	/	4113	481064	2111400

Figure 2. (a), (b) Transverse magnetic and (c), (d) electric fields simulated with the three different simulation methods at 63.94 MHz using the Fo8 RF coil in (a), (c) loaded and (b), (d) unloaded conditions.

It is shown that the simulation methods are all able to provide this kind of information. They all are useful for a posteriori simulation and also in the coil prototyping stage. None of the three methods can claim, in this case, a greater accuracy than the other. The main differences are: the number of mesh cells, the simulation time and the physical memory allocated during the simulation, as shown in Table 1. The average percentage difference between the maps is less than 1% in all cases, showing a substantial agreement between the results of the three simulation methods.

3.2. Dual Tuned RF Coil at 7 T

The second simulated model is a dual tuned ^{1}H/^{31}P RF coil for 7 Tesla MRI and MRS, in the unloaded and loaded conditions. In this case the geometry is simple but the wavelength is shorter (1 m) if compared to the electrical length of the coil. The load is positioned as shown in Figure 3. The results are reported in Table 2.

Regarding the tuning prediction, the agreement between the simulation and the measure is worse than for the Fo8, but it is still very good for most of the applications (within 6%). The time domain simulation gives better frequency prediction. Concerning the matching condition, the frequency domain results are in excellent agreement with the measurements, whereas some residual discrepancy is present for the FIT simulation. The isolation between the channels is predicted

Table 2. Comparison between measurements and simulations for the dual-tuned RF coil. The tuning and matching of both channels and decoupling between channels are reported.

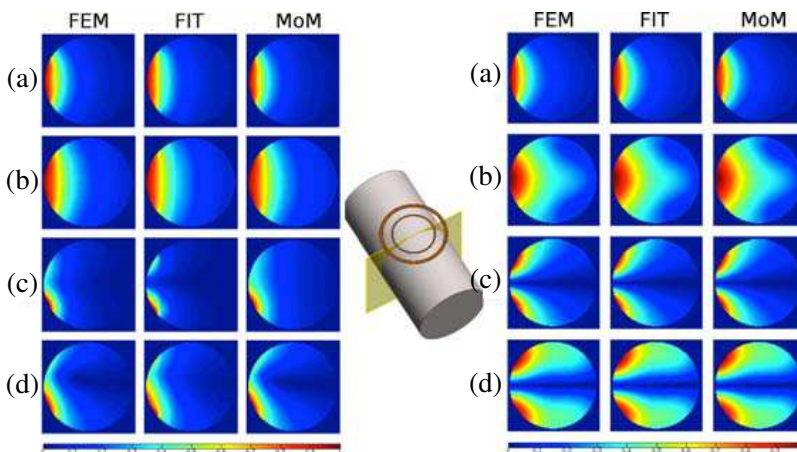| Quantity	Measure	MoM	FEM	FIT
Frequency, ^{1}H	298.6 MHz	6%	4%	2%
Matching, ^{1}H	−47 dB	0.4%	1%	10%
Frequency, ^{31}P	120.5 MHz	5%	5%	4%
Matching, ^{31}P	−24 dB	0.1%	1%	2%
Isolation at ^{1}H freq	−65 dB	0.01%	0.01%	0.01%
Isolation at ^{31}P freq	−13 dB	0.2%	1%	0.6%
Simulation time	/	15 min	2 h 57 min	18 h 49 min
Peak RAM used	/	1.6 Gb	8.09 Gb	1.03 Gb
No. mesh cells	/	3828	524496	1655280

Figure 3. (a), (b) Transverse magnetic field simulated at 120.6 MHz (^{31}P Larmor frequency) and 298.0 MHz (^{1}H Larmor frequency) respectively on a transverse plane; (c), (d) Electric field simulated at 120.6 MHz and at 298.0 MHz respectively on a transverse plane: the left and right images are referred to the unloaded condition and loaded condition respectively.

almost exactly by the three methods. Again, the main difference for the S parameter simulation is in the required run time and memory.

RF magnetic and electric simulated fields are shown in Figure 3. In the quantitative analysis, the average percentage difference between the field maps is always less than 1%. All the methods are able to

highlight the effect of the sample loading at high frequency (as can be inferred comparing Figure 3 left and right panels), which is one of the most important reasons for using a numerical simulation [8].

3.3. TEM Coil at 7 T

The third simulated model is a TEM volume coil for 7 T MRI. From a theoretical point of view, we expect a number of resonances proportional to the number of legs of the TEM coil. Each mode corresponds to a different phase of the RF current in the legs. In particular, for the lowest frequency mode ($M = 0$) the currents are all with the same phase and amplitude, while for the highest frequency mode ($M = 8$) the currents are $180°$ phase shifted between nearest elements. The remaining modes follow sinusoidal current distributions around the azimuthal angle, with increasing periodicity with the mode order. The mode $M = 1$ is therefore the fundamental one, corresponding to a sinusoidal current distribution with periodicity 2π and it generates a homogeneous transverse field inside the TEM coil. The $M = 1$ mode is the only one with a non-zero magnetic field at the center of the coil and this is the useful mode for MRI applications.

The simulation has been performed for the unloaded case only. In this context, the frequencies of the resonant modes and the corresponding E and H field distributions have been investigated. The reason for treating the unloaded case only is that we wanted to compare the capability of different numerical methods in calculating the E and H fields predicted by the theory [3]. Moreover, memory requirements are very demanding and the inclusion of the load will further increase them.

Most of the memory requirement is due to the meshing of tube legs used in the volume resonator under study: using copper strips rather than tube legs will lead to a decrease of memory requirement. The TEM coil simulation could be considered the worst case, being the geometric features of the model very demanding.

The measurement of S_{11} has been performed using a very small (0.1 pF) capacitor connected in series with the feeding coaxial cable, so to reduce perturbations due to the feeding itself. This feeding configuration can be reproduced with FEKO but not with CST. Thus, feeding in CST is modeled by connecting the port directly to the coil. In this way it is still possible to evaluate the frequencies of the resonant modes; however, their field distributions will be perturbed by the feeding port itself.

The resonant mode frequencies obtained by using the MoM and the FEM are shown in Table 3, together with measurements.

Table 3. Comparison between the simulated and measured frequencies for the TEM RF coil spectrum with the MoM and FEM methods.

Quantity	Measure	MoM	FEM
Frequency $M = 0$	275 MHz	358 MHz	349 MHz
Frequency $M = 1$	290 MHz	376 MHz	347 MHz
Frequency $M = 2$	305 MHz	401 MHz	396 MHz
Frequency $M = 3$	320 MHz	419 MHz	415 MHz
Frequency $M = 4$	333 MHz	437 MHz	429 MHz
Frequency $M = 5$	347 MHz	447 MHz	440 MHz
Frequency $M = 6$	358 MHz	458 MHz	447 MHz
Frequency $M = 7$	366 MHz	461 MHz	451 MHz
Frequency $M = 8$	371 MHz	463 MHz	/
Simulation time	/	13 h	12 h
Peak RAM used	/	12 Gb	16.5 Gb
No. mesh cells	/	18588	997164

The FIT simulation showed convergence problems: specifically, some preliminary tests leaded to an S_{11} with ripples even after more than 72 hours of simulations, while other preliminary tests failed to achieve condition on energy convergence. However, even if the convergence was not achieved, a good agreement with FEM has been noticed. These problems might be addressed through a mesh refining that should be handled by a more powerful computing resource, i.e., CPU cluster or GPU units.

In all the simulations it is possible to note a shift towards higher frequencies of the resonant modes; this shift can be presumably related to a coarse meshing of the tube legs and to the feed reactance, not properly taken into account by numerical techniques; indeed, this is a common drawback normally encountered in antenna simulations. However, for the two simulations the spacing between modes is in a very good agreement with the measured ones (relative error $< 5\%$). Moreover, it can be noticed that all the simulations are in good agreement between them, despite FEM cannot predict the last mode ($M = 8$) because of its low amplitude.

Concerning the E and H field simulations, in Figure 4, the magnetic and electric fields corresponding to the first 3 modes for the MoM and FEM simulations are shown.

The fields predicted by MoM are in qualitative agreement with the analytical theory of the TEM coil [3]. For example, we can notice that for modes $M = 0$ and $M = 2$ the magnetic field is zero in the
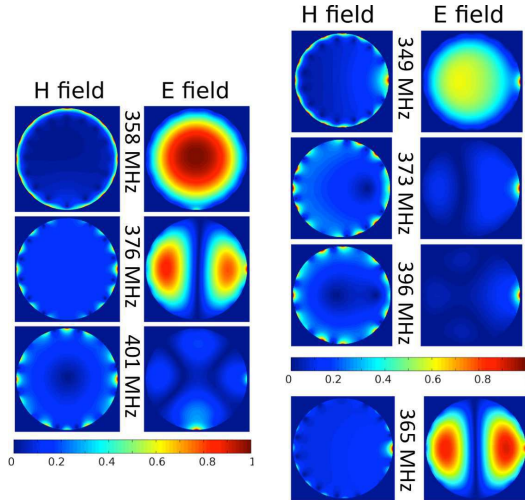
Figure 4. Transverse magnetic and electric fields for the unloaded TEM coil at the resonant frequency of the first 3 modes, obtained with MoM (left panel), with FEM (upper right) and off resonance e.m. fields for the $M = 1$ mode obtained with FEM (bottom right). The fields have been calculated in a plane perpendicular to the TEM axis and corresponding to the central section.

center of the coil, while it is homogeneous and different from zero for the $M = 1$ mode. Conversely, the results obtained by using FEM differ from the theoretical ones of the TEM coil because of the feeding perturbation. As explained above, it is not possible to add the series capacitors to the feeding port and this perturbes the field distribution. The perturbation of the feeding port can be reduced by calculating the field at a frequency which differs slightly from the resonant one.

As shown in Figure 4 the fields calculated at slightly off the resonant frequency of mode $M = 1$ are in good agreement with the results predicted through MoM.

Concerning the simulation time, MoM and FEM are almost equivalent, i.e., 13 and 12 hours, respectively.

It is worthwhile pointing out that running all the simulations on GPUs will lead to a strong reduction in simulation time. In case of MoM this is not valid since only the inversion of the matrix (and not the Z matrix filling) is implemented on GPU with FEKO 6.2. Therefore we decided to run all the simulations on CPU, to have a reliable comparison of the simulation times.

4. CONCLUSIONS

A quantitative comparison of performances and a detailed evaluation of advantages and drawbacks of the MoM, FEM, FIT methods is provided in this paper. Specifically, three coils which can be representative of different situations have been analyzed: a 1.5 T proton surface coil, a 7 T dual tuned surface coil and a 7 T proton volume coil.

Concerning the surface coils, we observed an excellent agreement in the prediction of the conditions of tuning and matching conditions between the measurements and the three numerical methods. More in detail, for the Fo8 coil at 1.5 T the MoM method provided the best agreement whereas for the dual tuned coil at 7 T the best agreement has been obtained by FIT. Concerning the magnetic end electric field maps, the average difference between the methods is less than 1% in all cases, showing an excellent agreement between the results of the MoM, FEM and FIT. All the three methods are able to provide accurate results, and to highlight the effect of the sample at high frequency. However, there are substantial differences in the time length of the simulation and in the amount of memory allocated. The MoM is faster and can be usefully applied when a homogeneous load is considered. The FIT simulation requires much longer time; but, if a inhomogeneous humanoid sample is considered as load, it can be successfully used. We can therefore conclude that, for this geometries, the frequency domain methods, especially MoM, are suitable for simulations performed in the prototyping stage, as they allow a fast computation, whereas the FIT is more suitable for a simulation aimed at evaluating the SAR and magnetic field inside a complex humanoid sample (at the expense of an increased duration of the simulation).

Concerning the volume TEM coil at 7 T, the simulation has been performed for the unloaded case only. The resonant modes frequencies obtained through MoM and FEM are in excellent agreement. In all the simulations it is possible to note a shift towards higher values of the resonant frequencies when compared with measurements. This shift can be presumably related to a relatively coarse meshing of the tube legs. However, for the two methods the spacing between modes is in a very good agreement with the measured one (relative error $< 5\%$), but FEM cannot predict the last mode ($M = 8$). Concerning the magnetic and electric field maps, the results obtained by using FEM are perturbed by the feeding port itself. The perturbation of the feeding port can be reduced by calculating the field at a frequency which differs slightly from the resonant one. MoM and FEM are almost equivalent in simulation time, i.e., 13 and 12 hours respectively.

In conclusion, the use of a range of simulation methods showed to

be a useful tool in the design and testing of RF surface and volume coils for both low and high-field MRI/MRS applications.

ACKNOWLEDGMENT

REFERENCES

1. Hayes, C. E., W. A. Edelstein, J. F. Schenk, O. M. Mueller, and M. Eash, "An efficient, highly homogeneous radiofrequency coil for whole-body NMR imaging at 1.5 T," *J. Magn. Reson.*, Vol. 63, 622–628, 1985.

2. Tropp, J., "The theory of the birdcage resonator," *J. Magn. Reson.*, Vol. 82, 51–62, 1989.

3. Vaughan, J. T., H. P. Hetherington, J. O. Out, J. W. Pan, and G. M. Pohost, "High frequency volume coils for NMR imaging and spectroscopy," *Magn. Reson. Med.*, Vol. 32, 622–628, 1994.

4. Alfonsetti, M., T. Mazza, and M. Alecci, "Optimization of multi-element transverse field radio frequency surface coils," *Magn. Reson. Mater. Phy.*, Vol. 17, No. 53, 2006.

5. Alfonsetti, M., V. Clementi, S. Iotti, G. Placidi, R. Lodi, B. Barbiroli, A. Sotgiu, and M. Alecci, "Versatile coil design and positioning of transverse-field RF surface coils for clinical 1.5 T MRI applications," *MAGMA*, Vol. 18, 69–75, 2005.

6. Alecci, M., S. Romanzetti, J. Kaffanke, A. Celik, H. P. Wegener, and N. J. Shah, "Practical design of a 4 Tesla double-tuned RF surface coil for interleaved 1H and 23Na MRI of rat brain," *J. Magn. Reson.*, Vol. 181, No. 2, 203–211, 2006.

7. Tropp, J., "Image brightening in samples of high dielectric constant," *Magn. Reson. Med.*, Vol. 167, 12–24, 2004.

8. Alecci, M., C. M. Collins, M. B. Smith, and P. Jezzard, "Radio frequency magnetic field mapping of a 3 Tesla birdcage coil: Experimental and theoretical dependence on sample properties," *Magnetic Resonance in Medicine*, Vol. 46, No. 2, 379–385, 2001.

9. Jin, J. M., "Electromagnetics in magnetic resonance imaging," *IEEE Antennas and Propagation Magazine*, Vol. 40, No. 6, 7–22, 1998.

10. Collins, C. M., S. Li, and M. B. Smith, "SAR and RF field distributions in a heterogeneous human head model within a birdcage coil," *Magn. Reson. Med.*, Vol. 40, 847–856, 1998.

11. Chen, J., Z. Fenga, and J. M. Jin, "Numerical simulation of SAR and B1-field inhomogeneity of shielded RF coils loaded with the human head," *IEEE Trans. Biomed. Eng.*, Vol. 45, No. 5, 650–659, 1998.

12. Ibrahim, T. S., R. Lee, B. A. Baertlein, A. Kangarlu, and P. M. L. Robitaille, "On the physical feasibility of achieving linear polarization at high field: A study of the birdcage coil," *Proc. Int. Soc. Magn. Reson. Med.*, Vol. 1, 2058, 1999.

13. Ibrahim, T. S., "Ultrahigh-field MRI whole-slice and localized RF field excitations using the same RF transmit array," *IEEE Transactions on Medical Imaging*, Vol. 25, No. 10, 1341–1347, 2006.

14. Simunic, D., P. Wach, W. Renhart, and R. Stollberg, "Spatial distribution of high-frequency electromagnetic energy in human head during MRI: Numerical results and measurements," *IEEE Trans. Biomed. Eng.*, Vol. 43, No. 1, 88–94, 1906.

15. Singerman, R. W., T. J. Denison, H. Wen, and R. S. Balaban, "Simulation of B_1 field distribution and intrinsic signal-to-noise in cardiac MRI as a function of static magnetic field," *J. Magn. Reson.*, Vol. 125, 78–83, 1997.

16. Mohsin, S. A., "A simple EM model for determining the scattered magnetic resonance radiofrequency field of an implanted medical device," *Progress In Electromagnetics Research M*, Vol. 14, 1–14, 2010.

17. Fuijita, H., L. S. Petropoulus, M. A. Morich, S. M. Shvartsman, and R. W. Brown, "A hybrid inverse approach applied to the design of lumped-element RF coils," *IEEE Trans. Biomed. Eng.*, Vol. 46, No. 3, 353–361, 1999.

18. Rogovich, A., A. Monorchio, P. Nepa, G. Manara, G. Giovannetti, and L. Landini, "Design of magnetic resonance imaging (MRI) RF coils by using the method of moments," *IEEE Antennas and Propagation Society International Symposium*, Vol. 1, 950–953, 2004.

19. Attardo, E. A., T. Isernia, and G. Vecchi, "Field synthesis in inhomogeneous media: Joint control of polarization, uniformity and SAR in MRI B_1-field," *Progress In Electromagnetics Research*, Vol. 118, 355–377, 2011.

20. Yau, D. and S. Crozier, "A genetic algorithm/method of moments approach to the optimization of an RF coil for MRI applications

— Theoretical considerations," *Progress In Electromagnetics Research*, Vol. 39, 177–192, 2003.

21. Collins, C. M., "Numerical field calculations considering the human subject for engineering and safety assurance in MRI," *NMR Biomed.*, Vol. 22, 919–926, 2009.

22. Hartwig, V., N. Vanello, G. Giovannetti, D. De Marchi, M. Lombardi, L. Landini, and M. F. Santarelli, "B_1+/actual flip angle and reception sensitivity mapping methods: Simulation and comparison," *Magn. Reson. Imaging*, Vol. 29, No. 5, 717–722, 2011.

23. Reza, S., S. Vijayakumar, M. Limkeman, F. Huang, and C. Saylor, "SAR simulation and the effect of mode coupling in a birdcage resonator," *Concepts in Magnetic Resonance Part B: Magnetic Resonance Engineering*, Vol. 31B, No. 3, 2007.

24. Weiland, T., "Time domain electromagnetic field computation with finite difference methods," *International Journal of Numerical Modeling: Electronic Networks, Devices and Fields*, Vol. 9, 295–319, 1995.

25. Yee, K. S., "Numerical solution of initial boundary value problems involving Maxwell's equations in isotropic media," *IEEE Trans. on Antennas and Propagat.*, Vol. 14, 302–307, 1966.

26. Peterson, A. F., S. L. Ray, and R. Mittra, *Computational Methods for Electromagnetics*, IEEE Press, New York, 1998.

27. Bérenger, J. P., "Three-dimensional perfectly matched layer for the absorprtion of electromagnetic waves," *Journal of Computational Physics*, Vol. 127, 363–379, 1996.

28. Mispelter, J., M. Lupu, and A. Briguet, *NMR Probeheads for Biophysical and Biomedical Experiments: Theoretical Principles and Practical Guidelines*, Imperial College Press, 2006.